

Springback Analysis and Optimization in Sheet Metal Forming

Abdulaziz Alghtani, P.C. Brooks, D.C. Barton, V.V. Toropov

Institute of Engineering Systems and Design, School of Mechanical Engineering
University of Leeds, Leeds LS2 9JT, UK

Abstract

An accurate prediction of springback in sheet metal forming processes requires complex hardening material models. In this research, numerical analysis of the springback in U-bending was conducted using the well-known Yoshida model, available and known as the YU model in LS-DYNA. This model has seven main parameters which describe the behaviour of the material as it undergoes metal forming processes. Initially, mesh sensitivity studies were conducted to derive a suitable mesh that represents an appropriate compromise between accuracy and computer time. Secondly design of experiment (DoE) was employed to make 30 combinations of two design variables (die radius and clearance) uniformly through a design space. Parametric optimisation studies were also conducted to investigate the influence of these variables and to make recommendations to minimise the springback. The results show that the blank element mesh density has a significant effect on the springback prediction. Additionally the results demonstrate that certain geometrical parameters have a significant impact in controlling the springback but that optimised values can be identified to minimise the effect.

1 Introduction

Sheet metal forming processes are widely used in the automobile industry. The most frequently used techniques are bending, stretching, stamping and other. In these sheet metal forming processes, defects such as rupture, wrinkling, galling and springback in formed parts might occur, whether during or after the process. The springback phenomenon is the most complex and challenging issue in industry. It is defined when the sheet metal is removed from the tools, the formed part tends to return to its original shape [1].

Over the last decades, many researchers have investigated the springback phenomenon in sheet metal forming processes. In particular Yoshida and Uemori have improved a model of large strain plasticity to predict more precisely the springback in sheet metal forming [2].

There are several factors that can control the springback in deformed sheet such as blank material properties, tooling configuration and/or process conditions [3]. For example, researchers have investigated the influence of die radius and clearance on springback of a deformed steel sheet [4, 5]. Investigators have also examined the influence of lubrication and clearance in springback during the square cup deep drawing process [6].

In the past many researchers have investigated the process of elastic-plastic deformation and they proposed many models but within small deformation. Sheet metal forming involves large deformations followed by an attempt to return to the blank's natural shape describing as springback phenomena. Recently, some researchers mentioned that for a precise prediction of springback, the Bauschinger effect should be taken into the account[2]. Few researchers investigated experimentally large-strain cyclic plasticity[7] , while many papers have been published on reverse deformation after the plastic deformation [8, 9]. Recently, Yoshida has succeeded doing cyclic tension-compression deformation experiments for sheet metal at large strain[2]

The numerical model which describes the large deformation and nonlinear material behaviour is the main challenge of using any kind of simulation package for metal forming analysis. Many researchers have proposed models but most of them have short falls in a full description of material behaviour.

Some of these models are suitable for a small range of deformation and others do not take into the account the Bauschinger effect which is an essential aspect to predict springback phenomenon. In the last decade, good improvement in terms of a more precise prediction of springback has been achieved. Researchers have examined the influence of five different hardening models on springback prediction and they have concluded that the Yoshida model has achieved good agreement with experiment [10]. Therefore this model will be used in the present work to investigate the influence of certain geometrical parameters in the U-bending process which are the die radius and clearance and to optimize these parameters to minimize the springback.

In a typical optimization problem, selected result responses are optimized by determining the best combination of design variables located in the design space. The design of experiment (DoE) approach is used to gain an accurate approximation of response surface which is called. Simulation of every possible set of the combination of these variables is complex. In such situation meta-modelling is frequently used reported in [11]. The response surface method evaluates an objective function at several points in the design space to gain a good approximation [12]. Researchers have designed an optimum blank for sheet metal forming by using the interaction of high- and low fidelity models [13]. Other researchers have designed an optimization scheme to minimize the springback in L-bending [14]. They developed Gauss-Newton techniques by coupling the Abaqus/standard code with Python. In the present study the genetic algorithm method is used to optimize parameters to give the minimum springback in the U-bending process.

2 Numerical Analysis

2.1 Finite Element Model

The U- bending process model consists of a punch, die, blank and blank holder. The whole assembly was modelled using 3-D quadratic shell elements as shown in Fig. 1. The punch, die and blank holder were considered to be rigid body while the blank was considered to be a deformable body. The baseline geometrical parameters are listed in Table 1.

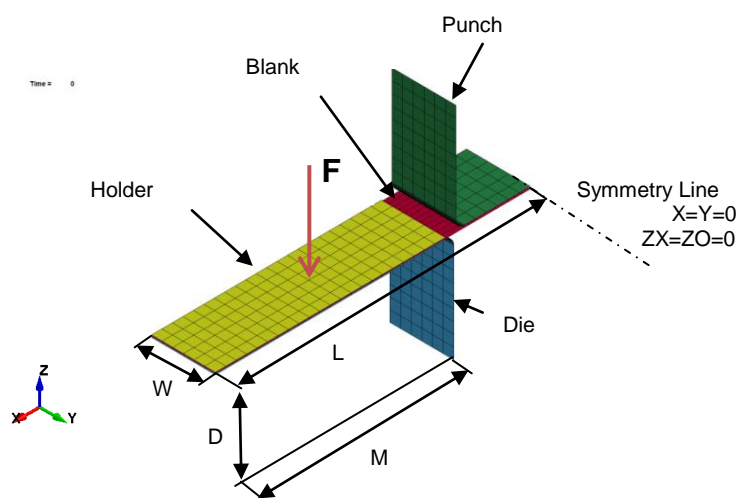


Fig. 1: U-Bending Model

Table 1: Dimensions of the U-bending model

Geometrical Parameters	L	D	W	M	Die radius (Dr)	Punch Radius (Pr)	Blank thickness	Clearance
Dimension (mm)	148	50	30	112	4	4	1	1.4

2.2 Material model

Many commercial FE codes gain constitutive model to simulate the mechanical behaviour of different materials. One of them is mixed isotropic-kinematic hardening model. Another one is by adding a linear component to the previous model. However, these models have limitations in predicting some aspects of material behaviour. For example Bauschinger effect, workhardening stagnation; when the rate of workhardening during large deformation is almost zero, and the reduction in Young's modulus in the case of unloading[2]. Also some researchers have suggested constitutive models which describes both Bauschinger effect, and workhardening stagnation [15]. However, they do not pay much effort to stress-strain responses in the small scale re-yielding region which is essential to predict the springback[2].

In the recent past, Yoshida and Uemori [2] have achieved a successful model that can precisely predict springback. This model consists of two surfaces: a yield surface and a bounding surface. The yield surface of the kinematic hardening model is surrounded by bounding surface of mixed isotropic-kinematic hardening as illustrated in Fig. 2. In the other word the yield surface is fixed in its size but its centre moves with the deformation as the bounding surface is allowed to be change in both size and location [2]. The yield function is expressed by:

$$f = \frac{3}{2}(s - \alpha):(s - \alpha) - Y^2 = 0 \quad (1)$$

where s and α are the Cauchy stress and the backstress, respectively. Y denotes the yield surface radius. The bounding surface expression is as follows:

$$F = \frac{3}{2}(s - \beta):(s - \beta) - (B + R)^2 = 0 \quad (2)$$

where β is the centre of bounding surface and $B+R$ is its initial size with R being associated with isotropic hardening.

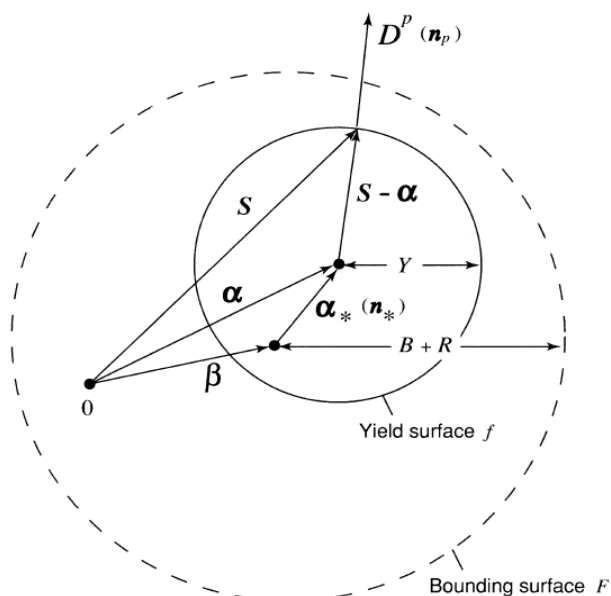


Fig. 2: Yoshida model of two surfaces [2]

This model contains seven material parameters (Y , C , B , R_{sat} , b , m , and h) where can experimentally be determined with help of some constitutive equations as follows:

1. Y is simply the radius of the yield surface which is the elastic limit.
2. B , $(R_{sat}+b)$ and m can be determined by equation (3) which comes from the evolution equation of the mixed isotropic- kinematic hardening of the bounding surface:

$$\sigma_{bound}^{(fow)} = B + R + \beta = B + (R_{sat} + b)(1 - e^{-m\epsilon^p}) \quad (3)$$

Here $\sigma_{bound}^{(fow)}$ denotes the yield stress of the bounding surface under uniaxial tension as shown in Fig. 3. R is the isotropic hardening stress and R_{sat} is the saturated value of the R at large plastic strain. m denotes the material parameter that controls the rate of isotropic hardening. b is also a material parameter. ϵ^p is plastic strain.

3 b is found using equation (4):

$$\sigma_{Bo}^{(p)} = 2\beta_o = 2b(1 - e^{-m\epsilon_o^p}) \quad (4)$$

Here, β_o is the kinematic hardening of the bounding surface at the point of reverse stress, see Fig. 3. ϵ_o^p denotes the plastic prestrain. From the experiment $\sigma_{Bo}^{(p)}$ can be obtained as shown in Fig. 3. and the parameter m is found in the step 2, then it is easy to find b by using equation (4)

4 Parameter C is determined from the stress strain curve of the transient Bauschinger deformation using

$$C \approx \frac{2}{\epsilon^p} \left[(1 + \ln 2) - \sqrt{\frac{|\alpha_*|}{a}} + \ln \left(1 + \operatorname{sgn}(\alpha_*) \sqrt{\frac{|\alpha_*|}{a}} \right) \right] \quad (5)$$

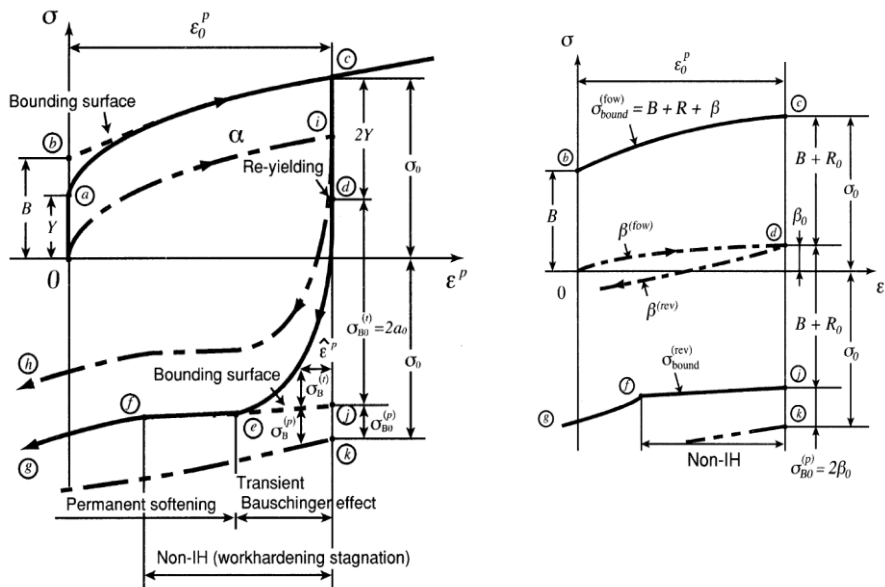


Fig. 3: The motion of a) The yield surface and b) The bounding surface under uniaxial forward-revers deformation [1]

5 h parameter is determined by simulations of the stress-strain response and it varies from 0 to 1.

Also in the Yoshida model, the effect of plastic strain on Young's modulus is taken into account by the following equation:

$$E = E_o - (E_o - E_a)(1 - e^{-\gamma p}) \quad (6)$$

Here E is Young's modulus and E_o and E_a are the Young's modulus for the original and for the plastic region, respectively. γ and p stand for a further material constant and the plastic strain respectively.

The material are used in this study is high strength steel DP600 and the parameters of the Yoshida model for this material are shown in Table 2 as reported in [16].

Table 2: The Yoshida model parameters for DP600 [16]

Y (MPa)	B (MPa)	Rsat (MPa)	b (MPa)	C	m	h	Eo (GPa)	Ea (GPa)	γ
360	435	255	66	200	26	0.4	206	152	61

2.3 Methods of analysis

The U-bending process consists of two sequential operations; loading and unloading. The loading process is initiated as the blank sheet is clamped by the blank holder. Then, the punch is moved down to draw the blank sheet into the die cavity making a U-shape. Subsequently, the unloading process can be defined when the work piece is freed from any constrains. Two types of analysis are typically used to solve this kind of process: explicit analysis for the large deformation forming operation and implicit analysis for the subsequent low deformation unloading operation leading to springback [17]

The boundary conditions assumed for this process were as follows:

1. The punch is constrained in all rotations and translations in both direction X and Y.
2. The blank holder is constrained in all rotation and displacements in both direction X and Y.
3. The die is fixed in all degrees of freedom.
4. The blank fixed along symmetry line in both x and y-direction for translation and ZX and ZO for rotation as shown in Fig. 1.

The punch is moved at a rate of 2 mm/ms in the Z-direction until it reaches the end of the operation which is at 50.5 mm of punch displacement. 50 kN load is applied on the middle of the blank holder in the Z-direction. A one way surface to surface contact was used to define the interaction between punch, die, and blank and blank holder components. In this contact definition, the blank holder, punch and die were considered as the master and the blank was considered to be the slave surface. Static and dynamic coefficients of friction were assumed to be 0.1.

In this study, the explicit method is firstly used to analyse the U-bending process. Then the implicit mode is utilized to calculate the springback that occurs in the blank during unloading process. In this implicit analysis, all constrains are removed from the workpiece so it is completely free to take up to its final deformation shape.

3 Mesh Sensitivity Study

3.1 Mesh definition

In finite element analysis, the mesh density is an important parameter to obtain accurate results. A small element size for discretisation of the blank provides precise results. On the other hand, the finer mesh leads to increased computation time. During the U- bending process, a certain area of the blank experiences much more severe stress than the rest. Moreover as the blank width is much bigger than its thickness, the effect of changing the mesh in the Y direction is negligible. Based on the above consideration, the blank has been divided into three areas designated A, B and C as shown in Fig. 4. The mesh size in region B is constant and minimum. Beyond zone B, the element size in zone A and C is increased slowly up to each free end. The element aspect ratio in zone B is set as shown in Fig. 4.

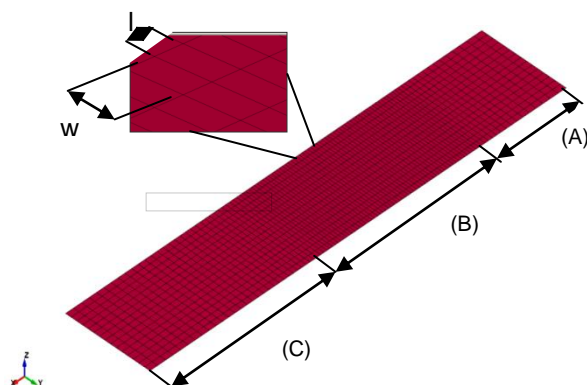


Fig. 4: The blank model for U-bending Simulation

The sensitivity of the results to the mesh density of the blank has been investigated to achieve a balance between the accuracy of the result and computation time. Table 3 shows the six different mesh sizes of the blank for the U-bending model.

Table 3: Different element size of the blank in U-bending and springback results

Mesh	l (mm)	w (mm)	Number of Elements	Elapse CPU time (hr : min : sec)		Springback	
				Forming (explicit)	Springback (implicit)	Θ_1	Θ_2
1	1.50	3.0	680	00:07:41	00:00:17	88.72	91.94
2	1.25	2.5	972	00:12:17	00:00:24	88.41	92.90
3	1.00	2.0	1530	00:31:25	00:00:35	87.83	94.12
4	0.75	1.5	2700	01:02:08	00:01:05	87.08	96.67
5	0.50	1.0	6090	03:31:29	00:02:54	86.57	97.54
6	0.25	0.5	24360	26:14:36	01:05:02	86.55	97.58

3.2 Punch Force prediction

The punch force versus its displacement has been plotted for the six different blank meshes as defined in Table 3. The trends are very similar for all meshes with slight differences in their behaviour. The punch force rises swiftly from the first contact point until it reaches almost 13 kN at 10 mm of punch travel. After that the punch force increases very slightly to the end of the operation.

Fig. 5 shows fluctuated forces for meshes 1-3 and Fig. 6 shows consistent trends with reasonable fluctuation for the last three blank meshes.

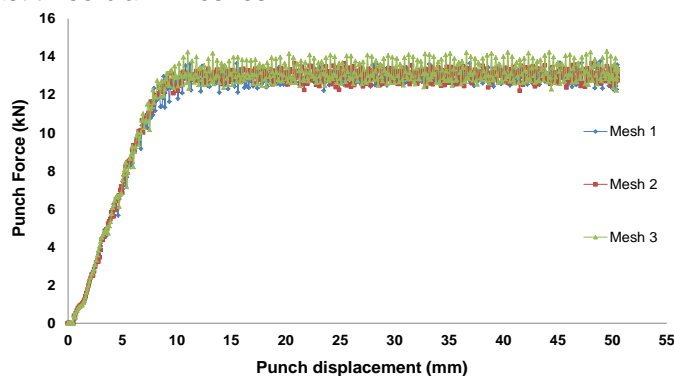


Fig. 5: Punch force versus displacement in U-bending process for meshes 1-3

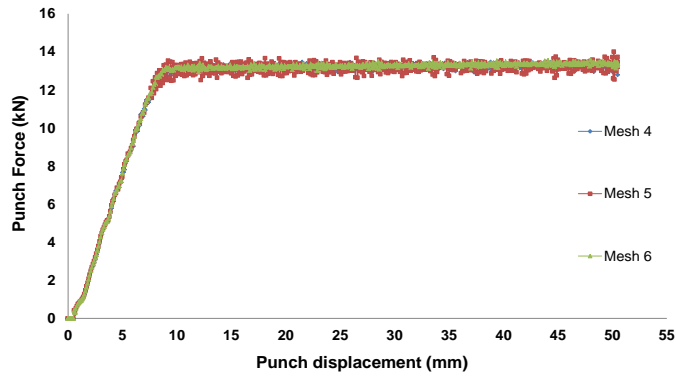


Fig. 6: Punch force versus displacement in U-bending process for meshes 4-6

3.3 Springback prediction

The springback in U-bending first is identified by measuring the maximum z-displacement of the blank flange after the forming operation [10, 18]. In some cases; the calculation of the springback by measuring the maximum-z displacement is not sufficient. Fig. 7 (a) shows almost the same maximum z-displacement along the top side of the U-shape. However, Fig. 7 (b) displays different z-displacement along the flange side of U-shape. Therefore the U-shape in both figures is different though the maximum z-displacement along the flange side is very similar.

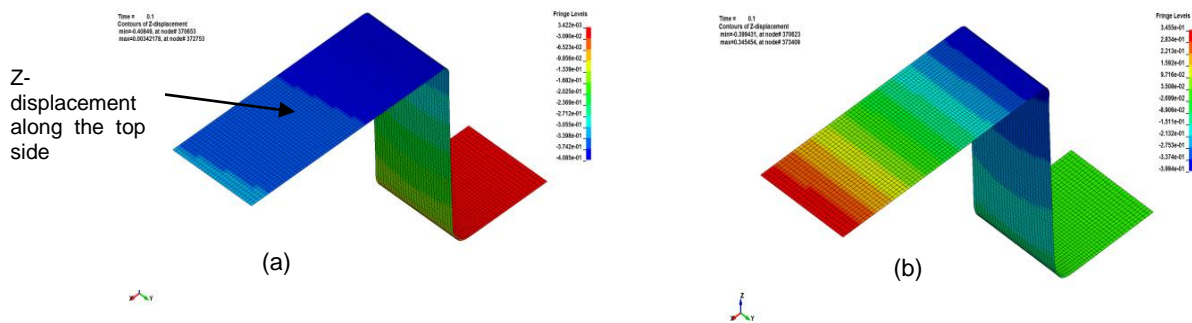


Fig. 7: Z-displacement for U-bending after the springback

Another approach for measuring the springback is by calculating the exact angle that follows the springback action [14, 19] as illustrated in Fig 8. Two angles are considered which are θ_1 and θ_2 . The angle of θ_1 is between line AB and CD, whilst θ_2 is identified as the angle between line CD and EF as can be seen in Fig 8. This study has utilized this second technique since it seems to be a more reliable methodology to measure the springback.

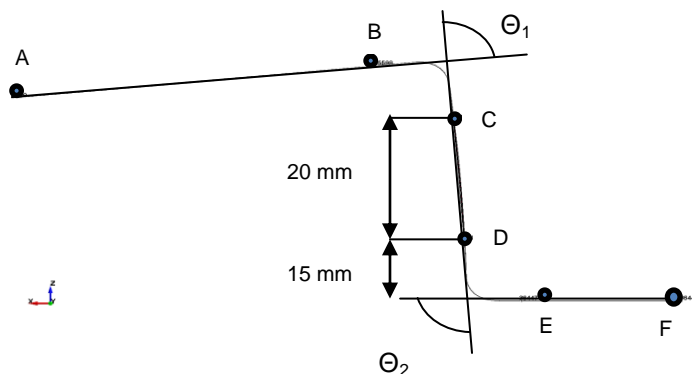


Fig 8: Springback angles (θ_1 and θ_2)

Table 3 shows a remarkable increase for θ_2 and slight decline for θ_1 from mesh 1 to mesh 4. However there is only a slight difference in the angles between mesh 5 and mesh 6 with a significant increase in elapse time for both the explicit (forming0 and implicit (springback) analyses. Therefore mesh 5 will be used for all further investigations.

4 Design of Experiments and Optimization

In a typical optimization problem, selected result responses are optimized by determining the best combination of design variables located within the design space. The location of the selecting points is important to gain an accurate approximation of the response surface. In this study, the Design of Experiments (DoEs) approach has been used to locate these points.

This study will investigate the influence of two design variables which are the die radius and clearance. Simulation of every possible set of the combination of these variables is complex. In such situations meta-modelling is frequently used [11]. This involves carrying out numerical analysis for certain combinations of design variables within a design space and fitting an approximate response surface to the actual results. In other words, the meta-modelling is used to provide an accurate response surface from a minimum number of simulations or experiments.

In this study, an Optimal Latin Hypercube (OLH) Design of Experiments (DoE) is used to make 30 combinations of the two design variables uniformly through a design space that is determined by the upper and lower limit for each variable. The DoE is divided into two parts; one is a build model and the second is a validation model. The purpose of each model is to maximize their uniformity taking account of the space-filling properties of the designs. As a result two non-overlapping DoEs are obtained which are the union of build points and validation points. There are several approaches to generate the OLH using criteria such as integrated mean squared error, maximizing entropy[20, 21] and maxi-min distance[22].

In this study, the PermGA algorithm reported in [11] is used to generate the OLH build and validation DoEs as uniformly as possible. This has the following physical meaning, the design space has points of mass unit and these points apply force on each other leading to a system that has a minimum potential energy. Using this method 30 combinations of the two design variables were uniformly distributed in a design space that is determined by upper and lower limit for each variable. The upper and lower limits for the two design variables are listed in Table 4. 30 points representing the combination set of die radius and clearance are uniformly distributed in the design space as shown in Fig. 9.

Table 4 Upper and lower limits for the two design variables

Variables	Upper)	Lower
Die Radius (mm)	10.7	2
Clearance (mm)	1.07	0.2

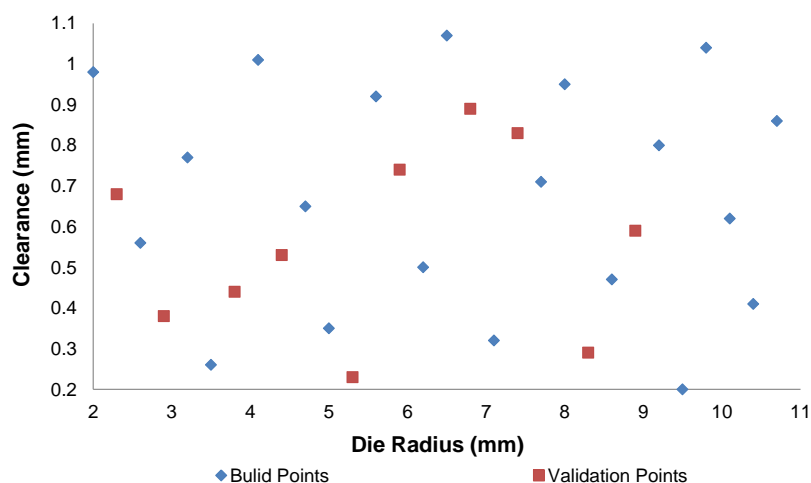


Fig. 9: Build and validation points

U-bending operations for the 30 selected points were simulated as described in section 2.3 using Ls Dyna software and the springback results are obtained. From this information, an approximation response surface of the springback within the design space was created using the moving least squares approximation method.

The response surface for the springback angles θ_1 and θ_2 is shown in Fig. 10 (a) and (b) respectively. Inspection of the thirty solutions showed that the die radius influences the springback angles much more than the clearance. The springback that represented by θ_2 shows that the springback increases dramatically with increase of the die radius. Interestingly the springback angle θ_1 has different behaviour with variation of the die radius. Fig. 10 (a) illustrated that the θ_1 is highest at the lower limit of the die radius (2 mm) followed by a sharp decrease up to 6 mm of die radius then the angle increases again to the upper die radius limit.

Finally the genetic algorithm GA optimization technique is employed using Hyperstudy v11 of Altair package. The main objective is to find optimal design variables that provides angles closet to 90 degrees or near. Table 5 shows the optimum design variables that leads to minimum springback angles. Also this table compares the predicted springback with the simulated one with mild error.

Table 5: Comparison of the predicted springback angles with the simulated one for the optimum design variables

Design variables		optimization		Simulation		Error %	
Die Radius (mm)	Clearance (mm)	θ_1	θ_2	θ_1	θ_2	θ_1	θ_2
2	0.245	91.755	91.707	92.162	92.141	0.43	0.54

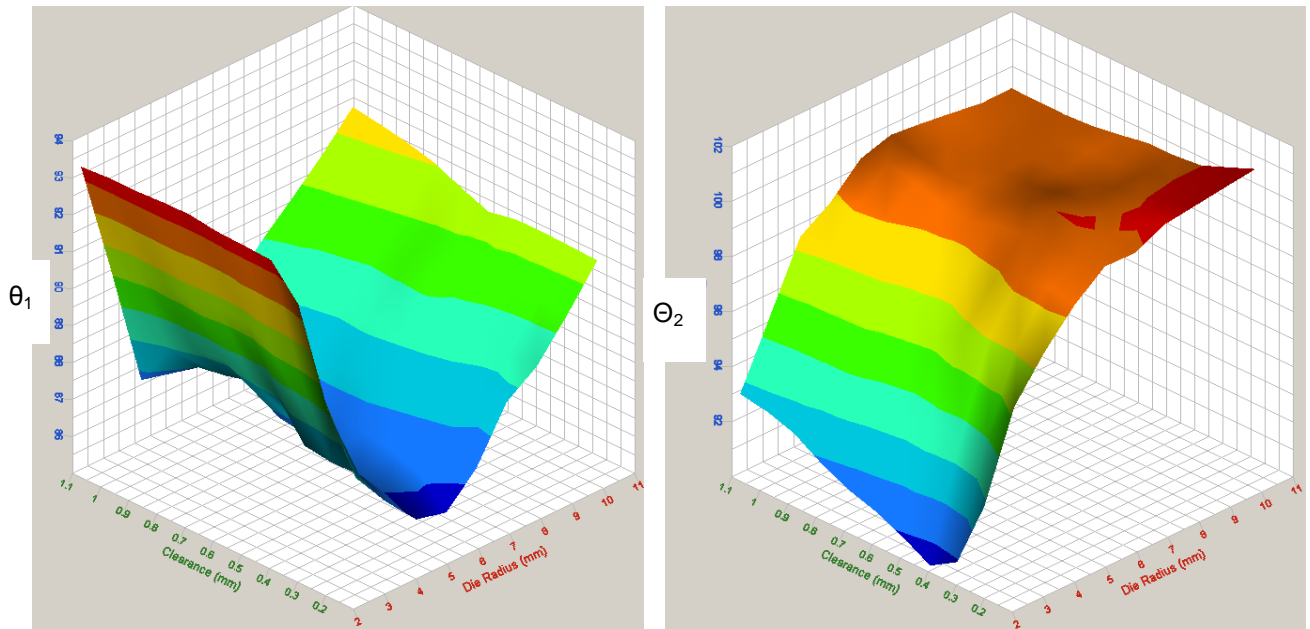


Fig. 10: Response surface of springback for a) θ_1 and b) θ_2

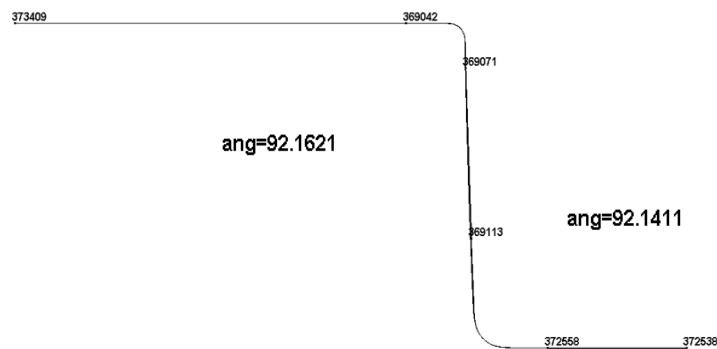


Fig. 11: The springback angles θ_1 and θ_2 for the optimum design variables

5 Conclusion

The numerical modelling of the U bending processes was developed using the Yoshida material model available in LS-DYNA. The mesh size of the deformable sheet is an important factor that influences the accuracy of the numerical results. Therefore this study conducted a mesh sensitivity study for the blank and selected an appropriate mesh size for the rest of the study. Important parameters such as die profile radius and clearance that influences the springback in U bending processes were investigated. A meta-modelling was used to generate suitable points of combination of die radius and clearance within the design space. These points were then simulated using LS-DYNA. It was found that the die radius influences the springback angles much more than the clearance. The GA optimization technique was employed using Hyperstudy version 11 to search for the optimum springback within the design space. It is demonstrated that the optimum springback is when the die radius and clearance equal to 2 mm and 0.245 mm respectively for the particular operation considered. These values of the design variables were then employed in LS-DYNA for validation purposes. The result showed that the springback is indeed minimized using this methodology.

References

1. Gau, J.-T. and G.L. Kinzel, *A new model for springback prediction in which the Bauschinger effect is considered*. International Journal of Mechanical Sciences, 2001. **43**(8): p. 1813-1832.
2. Yoshida, F. and T. Uemori, *A model of large-strain cyclic plasticity describing the Bauschinger effect and workhardening stagnation*. International Journal of Plasticity, 2002. **18**(5-6): p. 661-686.
3. Z. Marciniak, J.L.D.a.S.J.H., *Mechanics of Sheet Metal Forming*. 2002, Butterworth-Heinemann.
4. LIU, R.G.D.a.Y.C., *Control of Springback in a Flanging Operation*. APPLIED METALWORKING, 2 January 1984. **3**.
5. Chen, F.-K. and S.-F. Ko, *Deformation Analysis of Springback in L-Bending of Sheet Metal*. Advanced Science Letters, 2011. **4**(6-7): p. 1928-1932.
6. Lei, L.P., S.M. Hwang, and B.S. Kang, *Finite element analysis and design in stainless steel sheet forming and its experimental comparison*. Journal of Materials Processing Technology, 2001. **110**(1): p. 70-77.
7. Wilson, D.V. and P.S. Bate, *Reversibility in the work hardening of spheroidised steels*. Acta Metallurgica, 1986. **34**(6): p. 1107-1120.
8. Hasegawa, T., T. Yakou, and S. Karashima, *Deformation behaviour and dislocation structures upon stress reversal in polycrystalline aluminium*. Materials Science and Engineering, 1975. **20**(0): p. 267-276.
9. Christodoulou, N., O.T. Woo, and S.R. MacEwen, *Effect of stress reversals on the work hardening behaviour of polycrystalline copper*. Acta Metallurgica, 1986. **34**(8): p. 1553-1562.
10. Eggertsen, P.A. and K. Mattiasson, *On the modelling of the bending–unbending behaviour for accurate springback predictions*. International Journal of Mechanical Sciences, 2009. **51**(7): p. 547-563.
11. Narayanan, A., et al., *Simultaneous model building and validation with uniform designs of experiments*. Engineering Optimization, 2007. **39**(5): p. 497-512.
12. Mkaddem, A. and R. Bahloul, *Experimental and numerical optimisation of the sheet products geometry using response surface methodology*. Journal of Materials Processing Technology, 2007. **189**(1-3): p. 441-449.
13. Hino, R., F. Yoshida, and V.V. Toropov, *Optimum blank design for sheet metal forming based on the interaction of high- and low-fidelity FE models*. Archive of Applied Mechanics, 2006. **75**(10-12): p. 679-91.
14. Gassara, F., et al., *Optimization of springback in L-bending process using a coupled Abaqus/Python algorithm*. International Journal of Advanced Manufacturing Technology, 2009. **44**(1-2): p. 61-7.
15. Hu, Z., E.F. Rauch, and C. Teodosiu, *Work-hardening behavior of mild steel under stress reversal at large strains*. International Journal of Plasticity, 1992. **8**(7): p. 839-856.
16. Ninshu Ma, Y.U., Yuko Watanabe, Takaki Ogawa, *Springback Prediction by Yoshida-Uemori Model and Compensation of Tool Surface Using JSTAMP*. Numisheet 2008, 2008.
17. Prior, A.M., *Applications of implicit and explicit finite element techniques to metal forming*. Journal of Materials Processing Technology, 1994. **45**(1–4): p. 649-656.
18. Eggertsen, P.A. and K. Mattiasson, *On constitutive modeling for springback analysis*. International Journal of Mechanical Sciences, 2010. **52**(6): p. 804-818.
19. Chen, P. and M. Koç, *Simulation of springback variation in forming of advanced high strength steels*. Journal of Materials Processing Technology, 2007. **190**(1-3): p. 189-198.
20. Park, J.-S., *Optimal Latin-hypercube designs for computer experiments*. Journal of Statistical Planning and Inference, 1994. **39**(1): p. 95-111.
21. Ye, K.Q., W. Li, and A. Sudjianto, *Algorithmic construction of optimal symmetric Latin hypercube designs*. Journal of Statistical Planning and Inference, 2000. **90**(1): p. 145-159.
22. Johnson, M.E., L.M. Moore, and D. Ylvisaker, *Minimax and maximin distance designs*. Journal of Statistical Planning and Inference, 1990. **26**(2): p. 131-148.